



Electrochemical studies for the electroactivity of amine-capped aniline trimer on the anticorrosion effect of as-prepared polyimide coatings

Kuan-Yeh Huang^a, Yu-Sian Jhuo^a, Pei-Shan Wu^a, Chieh-Hisen Lin^a,
Yuan-Hsiang Yu^b, Jui-Ming Yeh^{a,*}

^a Department of Chemistry and Center for Nanotechnology at CYCU, Chung-Yuan Christian University, No. 200, Chung-Pei Road, Chung Li 32023, Taiwan, ROC

^b Department of Electronic Engineering, Lan-Yan Institute of Technology, I-Lan 261, Taiwan, ROC

ARTICLE INFO

Article history:

Received 12 March 2008

Received in revised form 21 October 2008

Accepted 24 October 2008

Available online 5 November 2008

Keywords:

Amine-capped

Aniline trimer

Electroactivity

Polyimide

Corrosion

ABSTRACT

The electroactive polyimide consisting of various content of amine-capped aniline trimers (ATs) have been successfully synthesized and characterized by Fourier-Transformation infrared and UV–visible absorption spectroscopy. The electroactivity of as-prepared polyimides was tested by electrochemical cyclic voltammetry (CV) studies. It was noticed that the as-prepared electroactive polyimide with higher content of amine-capped ATs shows higher electroactivity (i.e., larger redox current) than that of non-electroactive polyimide, leading to enhance corrosion protection efficiency on cold-rolled steel (CRS) electrodes. This enhanced corrosion protection efficiency has been explained based on a series of electrochemical measurements such as corrosion potential, polarization resistance, corrosion current and electrochemical impedance spectroscopy (EIS) studies in 5 wt-% NaCl electrolyte. This significant enhancement of corrosion protection on CRS electrodes as compared to non-electroactive polyimide might probably be attributed to the redox catalytic property of as-prepared electroactive polyimide coatings inducing the formation of passive layer of metal oxide.

© 2008 Elsevier Ltd. All rights reserved.

1. Introduction

Electroactive polymers have been classified as a new class of materials in the past decades and attracted extensive research activities due to it exhibited broad spectrum of potential commercial applications in electronic, optical, and biological research fields. Among those conducting polymers, polyaniline is a potential material for commercial applications due to its environmental stability, good processability and relatively low cost [1,2]. Polyanilines have lately drawn intensive attention from polymer scientists, physicists, and material scientists because of their widespread technological applications e.g., active electrode materials in energy-storage system [3,4], photo-electronic devices [5,6], sensors [7,8], gas separation membranes [9,10], anticorrosion coatings [11,12], antistatic [13] and electro-chromic materials [14,15].

Research activities have been focused particularly on the synthesis of aniline oligomers with well-defined structures and end-groups because of their good solubility and ability to undergo further polymerization. The synthesis of a number of aniline oligomers has been reported [16–21]. For example, Honzl and Tlustakova [19] prepared a series of phenyl-capped aniline oligomers with 2, 3, 4, and 6 amine units through complicated multi-step synthesis. In a landmark paper in 1986, Wudl et al. [20] reported the synthesis of phenyl-capped octaaniline by reacting tetraaniline with dihydroxyterephthalic acid. However, most synthetic routes of aniline oligomers involved multi-step reactions or the use of unstable reagents. Subsequently, Wei et al. [22] developed a convenient and one-step method to synthesize a series of aniline oligomers with well-defined structures and end-groups via chemical oxidation of aniline and its analogue compounds.

Recently, electroactive aniline oligomer-derivative polymers have evoked great research attentions [23–30].

* Corresponding author. Tel.: +886 3 2653341; fax: +886 3 2653399.
E-mail address: juiming@cycu.edu.tw (J.-M. Yeh).

For example, the preparation and electrochemical behavior of electroactive polyimide have been reported by Wang et al. [23,24] and Wei et al. [25]. On the other hand, the electrochemical behaviors of electroactive polyamide with amine-capped aniline pentamer prepared by oxidative coupling polymerization have also been demonstrated by Zhang and Wei et al. [26–29]. Furthermore, electroactive and biodegradable ABA type block copolymer of polylactide and aniline pentamer have been reported as scaffold materials for neuronal or cardiovascular tissue engineering [30]. However, the practical applications of electroactive aniline oligomer-derivative polymers such as electroactive polyimide, polyamide and epoxy resins have seldom been mentioned.

Oligomeric aromatic amines with amino groups at both ends are of great importance in polymer science and industries because of their applications as model compounds for electroactive polyanilines and as monomers to prepare polyamides, polyimides and epoxy resins. A general one-step approach was recently established by Wei et al. for the synthesis of aniline trimer from inexpensive materials [22]. Accordingly, trimer could be easily obtained in large quantity by oxidative coupling of *p*-phenylenediamine and aniline.

Therefore, in this work, we present first evaluations for the effect of amine-capped aniline trimer (AT) on the corrosion protection efficiency of as-prepared electroactive polyimide. First of all, the amine-capped ATs were synthesized by a one-step method from the oxidative coupling reactions of *p*-phenylenediamine with aniline in an acidic aqueous medium. The as-prepared AT molecules were characterized by mass spectroscopy (MS), Fourier-Transformation infrared (FTIR) and nuclear magnetic resonance (NMR) spectroscopy. Subsequently, a series of polyimides with different content of aniline trimer molecules were obtained by further reacted ATs with BSAA by thermal imidization at 200 °C. The as-prepared electroactive polymers were then characterized by FTIR and UV–visible absorption spectroscopy. The as-prepared polyimides were further identified by a series of electrochemical measurements such as corrosion potential (E_{corr}), polarization resistance (R_p), corrosion current (I_{corr}) and electrochemical impedance spectroscopy (EIS) studied in 5 wt-% NaCl electrolyte.

2. Experimental

2.1. Materials and instrumentations

Aniline (Sigma–Aldrich) was distilled prior to use. 4,4'-Oxydianiline (ODA; Fluka, Buchs, Switzerland), 1,4-phenylenediamine (Sigma–Aldrich), *N,N*-dimethylacetamide (DMAC); (Mallinckrodt/Baker, Paris, KY), 4,4'-(4,4'-isopropylidenediphenoxy)-bis(phthalic anhydride) (BSAA, Sigma–Aldrich, 97%) were used as received without further purification. All the reagents were reagent grade unless otherwise stated.

Mass spectra were run on a Bruker Daltonics IT mass spectrometer model Esquire 2000 (Leipzig, Germany) with an Agilent ESI source (model G1607-6001). Attenuated total reflectance FTIR were obtained with a FT/IR spectrometer (JASCO FT/IR-4100) at room temperature. ^1H NMR

spectra were run on a Bruker 300 spectrometer, referenced to internal standard of tetramethylsilane (TMS), DMSO was used as solvent. UV–visible absorption spectroscopy was obtained using a Hitachi U-2000 UV–visible spectrometer.

The passivating metal oxide layers were characterized by scanning electron microscopy (SEM), (Hitachi S-2300), and Electron Spectroscopy for Chemical Analysis (ESCA), (VG Scientific ESCALAB 250).

2.2. Synthesis of *N,N'*-bis(4'-aminophenyl)-1,4-quinonenediimine

A typical procedure was recently established by Wei et al. for the synthesis of the aniline trimer (AT) and accordingly, AT could be easily synthesized by oxidative coupling of 1,4-phenylenediamine and two equivalent amounts of aniline with ammonium persulfate as oxidant, as shown in Fig. 1 [22].

2.3. Synthesis of electroactive polyimide, electroactive copolyimide and non-electroactive polyimide

Three polyimides were prepared using 4,4'-oxydianiline (ODA), *N,N'*-bis(4'-aminophenyl)-1,4-quinonenediimine (aniline trimer), and 4,4'-(4,4'-isopropylidenediphenoxy) bis(phthalic anhydride) (BSAA) in different feed ratios. A typical procedure to prepare the electroactive polyimide is given as follows: BSAA (1.04 g, 2 mmol) was added to 6.0 g of DMAc at room temperature, with continuous stirring, for 30 min. A separate solution containing ATs (0.578 g, 2 mmol) in another 6 g of DMAc was prepared under mechanical stirring. After stirring for 30 min, both were subsequently mixed. The as-prepared mixture was then stirred for an additional 48 h at room temperature. It was subsequently poured onto the supporting substrate to form the electroactive polyimide and then dried under vacuum at 200 °C for 12 h. The synthesis procedure of electroactive polyimide is depicted in Fig. 1. Composition of the polyimide materials with respect to ATs content, as summarized in Table 1.

2.4. Electrochemical cyclic voltammetric (CV) studies on the electroactivity of as-prepared electroactive polyimide, copolyimide and non-electroactive polyimide

Electroactive experiments were performed on VoltaLab 40 (PGZ 301) analytical voltammeter using a conventional three-electrode system. All the CV measurements were performed at a double-wall jacketed cell, covered with a glass plate, through which water was circulated from a YEONG SHIH B-20 thermostat to maintain a constant operational temperature of 25 ± 0.5 °C. The as-prepared polyimide-film-coated electrode was prepared by casting the polymer solution in DMAc (0.25 M) on top of the working electrode and then drying it in air. The platinum foil (applied surface area = 1 cm^2) was acted as a working electrode, a platinum wire and saturated calomel electrode (SCE) were used as counter and reference electrode, respectively. The working electrode coated polyimide thin film and then scanned by potential cyclic between 0 and 0.9 V with a scan rate of 50 mV s^{-1} in 1 M H_2SO_4 . The electrochemical CV measure-

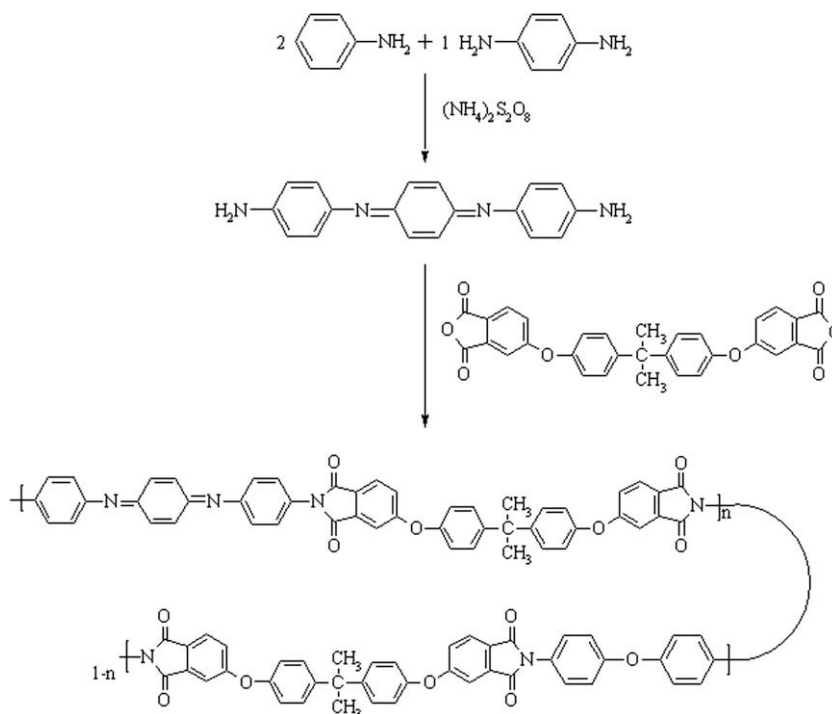


Fig. 1. Schematic representation of the synthesis of aniline trimers and polyimides.

Table 1

Feed composition ratio of electroactive polyimide, electroactive copolyimide, and non-electroactive polyimide with the E_{corr} , R_p , I_{corr} , and R_{corr} measured from electrochemical method.

Compound code	Feed composition (molar)			Electrochemical corrosion measurements					
	Diamine		Dianhydride	E_{corr} (mV)	R_p ($\text{k}\Omega \text{ cm}^2$)	I_{corr} ($\mu\text{A}/\text{cm}^2$)	R_{corr} (MPY)	Thickness (μm)	$P_{\text{EP}}\%$
	ODA	ATs	BSAA						
Bare ^a	–	–	–	–720	0.018	18.900	8.820	–	–
electroactive polyimide	0	1	1	–486.5	0.560	0.103	0.048	22	30.0
electroactive copolyimide	0.5	0.5	1	–592.2	0.246	0.400	0.187	20	12.6
Non-electroactive polyimide	1	0	1	–647.8	0.074	0.700	0.327	19	3.1

^a Pristine CRS used for test.

ments of all samples were repeated at least three times to ensure consistence.

2.5. Electrochemical corrosion evaluations of electroactive polyimide, copolyimide and non-electroactive polyimide

To measure the electrochemical corrosion performance of sample-coated CRS electrodes, a series of electroactive polyimides were first cast dropwisely onto the CRS coupons ($1.0 \times 1.0 \text{ cm}$), followed by drying in air at 200°C for 12 h for allowing the evaporation of solvent molecules to give a uniform and dense coatings of about $20 \pm 2 \mu\text{m}$ in thickness, measured by digimatic micrometer (Mitutoyo, Japan). The coated and uncoated coupons were then mounted to the working electrode so that only the coated side of the coupon was in direct contact with the electrolyte. The edges of the coupons were sealed with super fast epoxy cement (SPAR[®]). All the electrochemical corrosion measurements and impedance spectroscopy were

performed on a VoltaLab 21 (PGP 201) and repeated at least three times to ensure a reproducible result. All the electrochemical corrosion measurements were also performed at a double-wall jacketed cell, covered with a glass plate, through which water was circulated from a YEONG SHIH B-20 thermostat to maintain a constant operational temperature of $25 \pm 0.5^\circ\text{C}$. As electrolyte, aqueous solutions of NaCl (5 wt-%) were used. Open circuit potential (OCP) at the equilibrium state of the system was recorded as the corrosion potential (E_{corr} in mV versus SCE). Polarization resistance (R_p in Ω/cm^2) was measured by sweeping the applied potential from 20 mV below to 20 mV above the E_{corr} at a scan rate of 10 mV/min and recording the corresponding current change. R_p value was obtained from the slope of the potential-current plot. The Tafel plots were obtained by scanning the potential from 250 mV below to 250 mV above the E_{corr} at a scan rate of 10 mV/min. Corrosion current (I_{corr}) was determined through superimposing a straight line along the linear portion of the cathodic or

anodic curve and extrapolating it through E_{corr} . The corrosion rate (R_{corr} , in milli-inches per year, MPY) was calculated from the following equation:

$$R_{\text{corr}}(\text{MPY}) = [0.13I_{\text{corr}}(\text{E.W.})]/[A \cdot d]$$

where E.W. is the equivalent weight (in g/eq.), A is the area (cm^2) and d is the density (g/cm^3).

VoltaLab 40 (PGZ 301) potentiostat/galvanostat was employed to perform the a.c. impedance spectroscopy measurements. Impedance measurements were carried out in the frequency range of 100 K–100 mHz. The working electrode was first maintained in the test environment for 30 min before the impedance run. This step served to put the electrode in a reproducible initial state and to make sure that no blistering occurred during the conditioning period. All experiments were operated at room temperature. All raw data were repeated at least three times to ensure reproducibility and statistical significance.

2.6. Scotch tape test for the adhesive property

A simple Scotch tape test was used to estimate the relative adhesiveness of the coatings to the substrate. The coat-

ing on the CRS was cut with a razor to make grid lines. The total test area was 4.0 cm^2 with each square dimension of $2 \times 2 \text{ mm}$. Scotch tape (Scotch Magic tape with a width of 19.0 mm, by 3 M) was applied firmly to cover the grid area at room temperature. After about 1 min, the tape was stripped off with one quick peeling. By counting the number of squares peeled off versus the total number of squares covered under the tape, the relative adhesiveness of the films of the polyimide coatings can be estimated. For each sample, at least 3 three parallel tests were performed.

3. Results and discussion

3.1. Synthesis and characterization

3.1.1. Aniline trimer

The molecular weight of aniline trimer was characterized by matrix assisted laser desorption ionization time-of-flight mass spectroscopy. The MS detection was performed in the selected ion mode, affording pseudo-molecular ions in the form of M^+ or $(MH)^+$. From Fig. 2(a), we can see only the molecular ion peak appeared (i.e. 289 m/z for the aniline trimer). Moreover, in the FTIR spectrum (Fig. 2(b)) of the

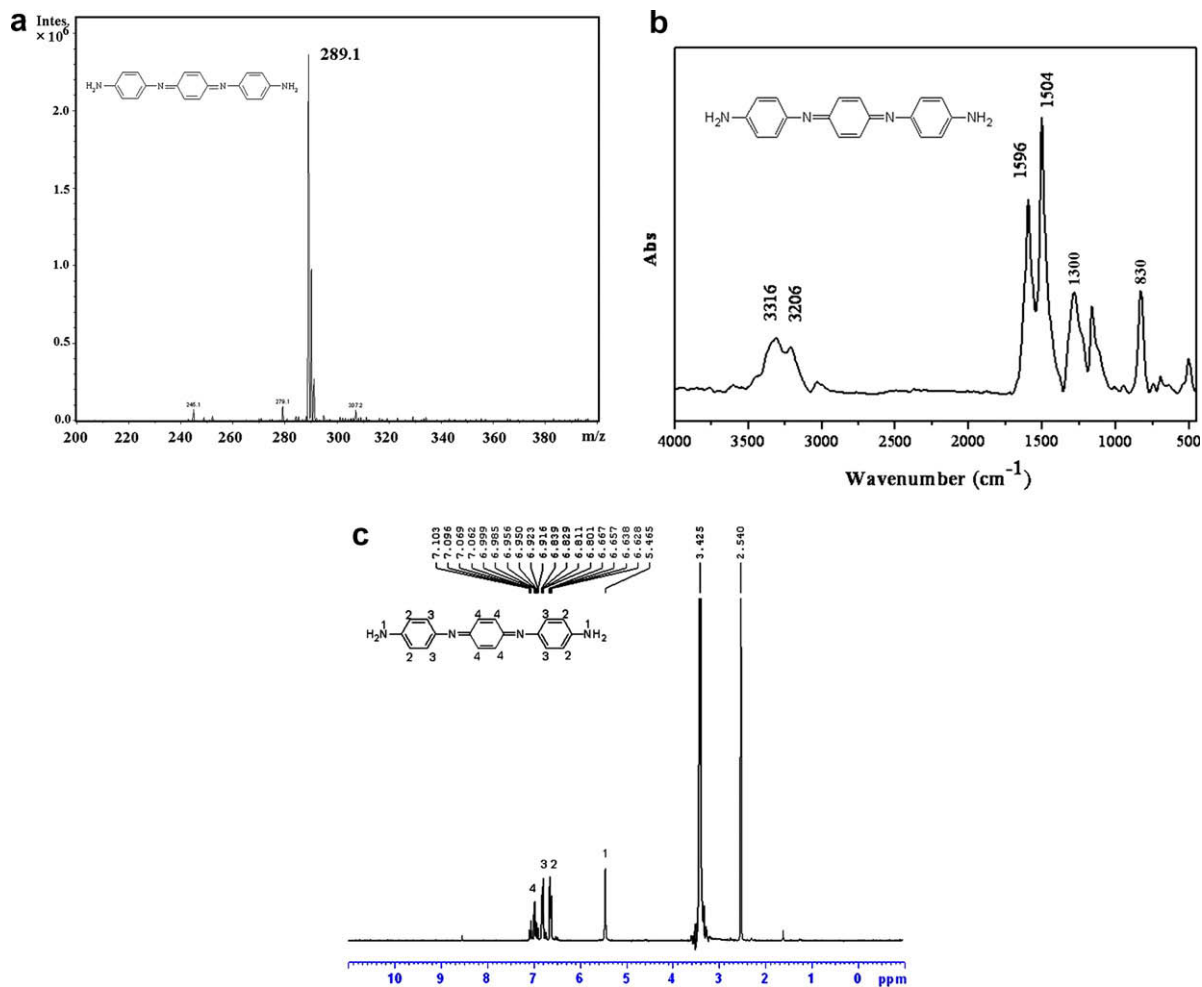


Fig. 2. Spectral studies on aniline trimer (a) MASS (b) FTIR and (c) ^1H NMR spectra.

aniline trimer, the characteristic absorption bands appeared at 3316 cm^{-1} and 3206 cm^{-1} arising from the terminal $-\text{NH}_2$ of aniline trimer are observed. The characteristic absorption peaks appeared at 1596 cm^{-1} and 1504 cm^{-1} were assigned to the vibrational bands of quinoid rings and benzenoid rings of aniline trimer, respectively. At 1300 and 830 cm^{-1} absorption peaks were characteristic of the aromatic N–H group, and the para substitution of benzene ring. For the NMR spectroscopy studies, signals at 5.50 ppm in the ^1H NMR spectrum (Fig. 2(c)) can be assigned to the primary amine protons ($-\text{NH}_2$) of ATs and the relative intensity of signals around $\delta = 7.35\text{--}6.50\text{ ppm}$ allow estimation of other expected splitting of the aromatic proton signals of aniline trimer.

3.1.2. Polyimide

Following a successful model reaction, three polyimides were prepared using 4,4'-oxydianiline (ODA), aniline trimer, and 4,4'-(4,4'-isopropylidenediphenoxy)-bis(phthalic anhydride) (BSAA) in different feed ratios. It was found that the stoichiometry of all monomers could be readily achieved by slow addition of diamine to the reaction medium upon observation of a significant increase in solution viscosity. All the copolymers were characterized by spectroscopic means (UV–vis and FTIR).

For the studies on FTIR spectroscopy, the electroactive polyimide prepared from thermal imidization of aniline trimer and BSAA exhibited an obvious carbonyl asymmetric stretching of $\nu_{\text{C=O}}$ located at 1850 and 1778 cm^{-1} and symmetric stretching of $\nu_{\text{C=O}}$ located at 1720 cm^{-1} , respectively. The characteristic peak near 738 cm^{-1} due to the imide ring deformation of electroactive polyimide was also found in the IR spectra. Moreover, the FTIR spectroscopy of electroactive copolyimide revealed a decrease in intensity ratio of $\nu_{\text{C=O}}$ (1850 cm^{-1})/ $\nu_{\text{C=O}}$ (1778 cm^{-1}), indicating decrease in feed composition ratio of aniline trimer/ODA existed in the as-prepared electroactive copolyimide and this ratio permits to estimate the extent of oxidation of the polymer. However, the non-electroactive polyimide have lack of characteristic asymmetric stretching of $\nu_{\text{C=O}}$ (1850 cm^{-1}) of aniline trimer, as shown in Fig. 3(a).

Moreover, for the UV–visible spectra studies on as-prepared polyimide, electroactive polyimide (Fig. 3(b) curve 1) and copolyimide (Fig. 3(b) curve 2) had a maximum absorbance (λ_{max}) at 324 nm , indicating the presence of the leuco aniline trimer or the 1,4-bis(phenylamino) benzene moiety in the polymer backbone [23]. However, the non-electroactive polyimide (Fig. 3(b) curve 3) exhibited no peak appeared at 324 nm , as shown in Fig. 3(b).

On the other hand, the results of the Scotch tape test are to estimate the adhesive property of the polyimide coating. In general, they were exhibited the good adhesive properties. All the polyimide coatings were almost intact completely when the tape was stripped off. It was further demonstrated to be fabricated by electrochemical test.

3.2. Electroactivity of electroactive copolyimide, polyimide coatings

Cyclic voltammetry (CV) has been widely used to characterize the electrochemical properties of electroactive

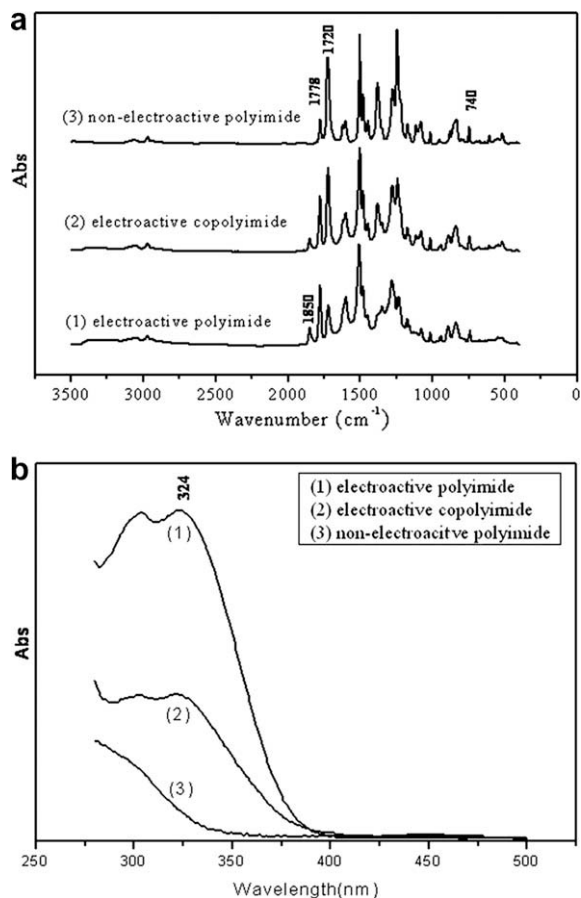


Fig. 3. Spectral studies on electroactive polyimide (1), electroactive copolyimide (2) non-electroactive polyimide (3) (a) attenuated total reflectance FTIR (b) UV–vis spectra.

polymers. In this paper, the polymers were characterized by CV using a three-electrode electrochemical cell. A thin film of polymer was formed by evaporation of a DMAc-polymer solution on the surface of the Pt working electrode. The CV experiment was carried out in 1.0 M aqueous sulfuric acid solution with a scan rate of 50 mV/s . The CV spectrum showed one oxidation peak at 0.53 V for electroactive polyimide (Fig. 4(a)), which is similar to many longer oligomers that undergo two electron transfer processes.

It should be noted that the electroactive polyimide having higher content of aniline trimer exhibited a larger redox current at 3.38 mA/cm^2 (i.e., higher electroactivity) as compared to that of electroactive copolyimide. However, non-electroactive polyimide showed null zero redox current. This implied that the incorporation of ATs into the polyimide may introduce the electroactivity into as-prepared polyimide. Moreover, the incorporation of higher AT content may yield a polyimide with higher electroactivity. We therefore envisioned that the electroactive polyimide in the form of coating may reveal an effectively enhanced corrosion protection effect, as similar to that of neat polyaniline, based on a series of electrochemical standard corrosion measurements (e.g., potentiodynamic and electrochemical impedance measurements) as discussed in the following sections.

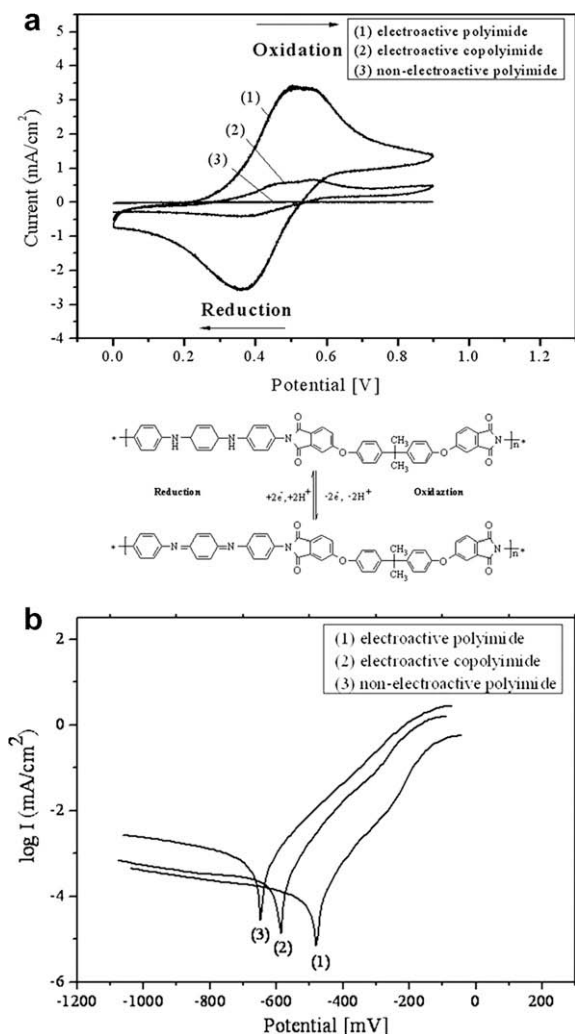


Fig. 4. (a) Cyclic voltammetry of the polyimide shown as (1) electroactive polyimide, (2) electroactive copolyimide, and (3) non-electroactive polyimide above were measured in aqueous H₂SO₄ (1.0 M) with scan rate of 50 mV/s. The proposed oxidation mechanism is shown below. (b) Tafel plots for (1) electroactive polyimide, (2) electroactive copolyimide, and (3) non-electroactive polyimide, measured in 5 wt-% aqueous NaCl solution.

3.2.1. Potentiodynamic measurements

In this section, corrosion protection effect on the CRS electrodes coated with a series of as-prepared polyimides can be evaluated by operating sequential electrochemical corrosion parameters such as E_{corr} , R_p , I_{corr} and corrosion rate (R_{corr}).

Generally, CRS electrodes coated with neat non-electroactive polyimide coating shows a higher E_{corr} value than the uncoated CRS electrode, which is consistent with previous observation on organic-based coating system [31]. However, it revealed a lower E_{corr} value than the specimen coated. For example, electroactive polyimide-coated CRS electrode exhibited a high corrosion potential of ca. -486.5 mV at running time of 30 min ($I_{\text{corr}} = 0.103$ $\mu\text{A}/\text{cm}^2$). Even after 5 h measurement, the potential remained at ca. -488.5 mV. Such E_{corr} value implies that the electro-

active copolyimide-coated CRS electrode is noble towards the electrochemical corrosion compared to the neat non-electroactive polyimides. Furthermore, the non-electroactive polyimide-coated CRS showed corrosion potential of -647.8 mV ($I_{\text{corr}} = 0.700$ $\mu\text{A}/\text{cm}^2$), which is significantly lower than that of electroactive polyimides with higher AT content displaying better corrosion protection performance on CRS electrode than that of low content of aniline trimer. The most anodic value of E_{corr} indicates that the electroactive polyimide-coated CRS electrode should have the highest corrosion protection. Therefore, this shift is related to transformation of emeraldine state of electroactive polyimide coating to the leucoemeraldine state corrosive solutions [32]. The polarization resistances, R_p , were evaluated from the Tafel plots, according to the Stern–Geary equation [33],

$$R_p = b_a b_c / 2.303 (b_a + b_c) I_{\text{corr}}$$

Here, I_{corr} is the corrosion current determined by an intersection of the linear portions of the anodic and cathodic curves, and b_a and b_c are anodic and cathodic Tafel slopes ($\Delta E/\Delta \log I$), respectively. The protection efficiency ($P_{\text{EF}\%}$) values were estimated using the following equation [34]:

$$P_{\text{EF}\%} = 100 [R_p^{-1}(\text{uncoated}) - R_p^{-1}(\text{coated})] / R_p^{-1}(\text{coated}).$$

The CRS electrodes coated with electroactive polyimides having higher content of aniline trimers showed a polarization resistance (R_p) value of $0.56 \times \text{k}\Omega/\text{cm}^2$ in 5 wt-% NaCl electrolyte, which is obviously greater than that of CRS electrode coated with electroactive copolyimides with lower content of aniline trimers ($R_p = 0.246$ $\text{k}\Omega/\text{cm}^2$). Tafel plot for (1) electroactive polyimide-coated (2) electroactive copolyimide-coated (3) non-electroactive polyimide-coated CRS electrodes are shown in Fig. 4(b). For example, the corrosion current (I_{corr}) of CRS electrode coated with electroactive polyimide is ca. 0.100 $\mu\text{A}/\text{cm}^2$, which is correspondent to a corrosion rate (R_{corr}) of ca. 0.048 millinches per year (MPY), which is significantly lower than that of non-electroactive polyimide (i.e., 0.700 $\mu\text{A}/\text{cm}^2$ and 0.327 MPY), as summarized in Table 1.

3.2.2. Electrochemical impedance measurements

Electrochemical impedance spectroscopy (EIS) was an alternative tool to evaluate the activity difference between surface of CRS electrode after un-electroactive polyimide, electroactive copolyimide and electroactive polyimide treatment. Impedance is a totally complex resistance when a current flows through a circuit made of capacitors, resistors, or insulators, or any combination of these [35]. EIS measurement results in currents over a wide range in frequency. For the electroactive polyimides, an analogue circuit (called a Randles circuit), as represented in upper part of Fig. 5(a) could be used, in which together with the above traditional components. It is made of a double-layer capacitor in parallel with a charge transfer resistor and connected in series with a electrolyte solution resistor. The impedance (Z) depends on the charge transfer resistance (R_{ct}), the solution resistance (R_s), the capacitance of the electrical double-layer or oxide film capacitance (C),

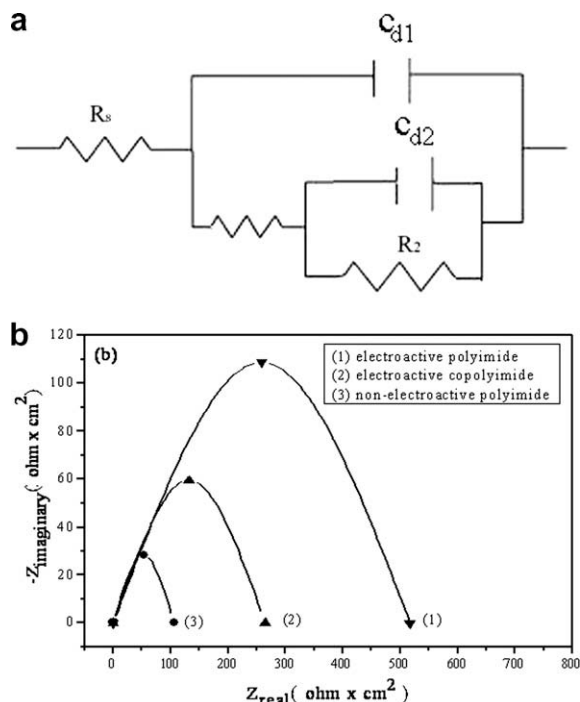


Fig. 5. (a) Analogue circuit, (b) Nyquist plots for (1) electroactive polyimide, (2) electroactive copolyimide, and (3) non-electroactive polyimide-coated CRS electrode, measured in 5 wt-% aqueous NaCl solution.

and the frequency of the AC signal (ω). It can be reduced as:

$$Z = Z' + jZ'' = R_s + R_{ct} / [1 + (R_{ct}C_{dl\omega})^2] + j(R_{ct}^2 C_{dl\omega}) / [1 + (R_{ct}C_{dl\omega})^2]$$

The high-frequency intercept is equal to the solution resistance, and the low-frequency intercept is equal to the sum of the solution and charge transfer resistances [36]. The higher the semicircle diameter (charge transfer resistance) the lower the corrosion rate [36,37].

A series of samples denoted with (1)–(3) were coated by electroactive polyimide, electroactive copolyimide and non-electroactive polyimide. The corrosion protection studies of these samples with $\sim 20 \pm 2 \mu\text{m}$ in coating thickness immersed in 5 wt-% aqueous NaCl electrolyte for 30 min was followed by EIS.

First of all, we found that the charge transfer resistance of samples as determined by the intersection of the low-frequency end of the semicircle arc with the real axis is 106.4, 264.8, and 517.6 $\text{k}\Omega \text{cm}^2$, respectively (Fig. 5(b)). This result clearly demonstrated that the sample, with the highest content of aniline trimer, has the greatest corrosion protection performance. It should be further noted that neat electroactive polyimide exhibited a higher charge transfer resistance (i.e., 517.6 $\text{k}\Omega \text{cm}^2$). According to the Fig. 5(b) (curve 3), the non-electroactive polyimide exhibits a charge transfer resistance of 106.4 $\text{k}\Omega \text{cm}^2$.

Furthermore, EIS Bode plots (impedance vs. frequency) of as-prepared electroactive polyimide are shown in Fig. 6. The increase of impedance value at high

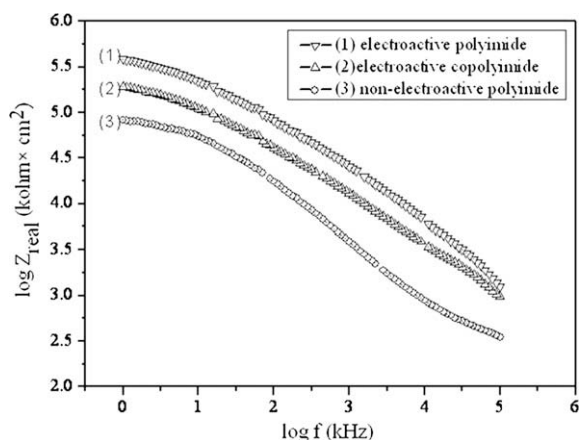


Fig. 6. Bode plots for (1) electroactive polyimide, (2) electroactive copolyimide, and (3) non-electroactive polyimide-coated CRS electrode, measured in 5 wt-% aqueous NaCl solution.

content of aniline trimer in the monitoring frequency region from low to high-frequency can be interpreted due to redox catalytic property of electroactive polyimide resulted from the aniline trimer. Again, the electroactive polyimide coating, exhibited a higher charge resistance than that of non-electroactive and electroactive copolyimides, in the entire monitoring frequency range base on the studies of EIS Bode plots. In conclusion, the enhancement of anticorrosive effect in electroactive polyimide, in the form of coating, compared to non-electroactive polyimide might be resulted from the passive layer of metal oxide induced by the electroactive redox catalytic property.

3.3. Observations and investigation on the CRS surface

Visual observation of the passivation oxide layers exhibited a grayish oxide layer form over the CRS surface under the electroactive polyimide and electroactive copolyimide coating on CRS. The as-prepared samples were stored 24 h at room temperature and then removed by razor knife. It is similar to what was observed by Wesling [38,39]. The SEM images revealed that the oxide layers was formed between the electroactive polyimide and electroactive copolyimide coating and the CRS surface (Fig. 7(b, and c)) but we could not observe the same image from the pure CRS surface (Fig. 7(a)).

In addition to the SEM observations, the chemical nature of the passivation oxide layers was measured by ESCA. The surface of CRS were first coated with the electroactive polyimide and electroactive copolyimide then exposed to a NaCl corrosion environment for a short period of time (24 h). Then the electroactive polyimide and electroactive copolyimide layer was removed and examined by ESCA. The Fe $2p_{3/2}$ peak binding energy of Fe_2O_3 is 710.9 eV; FeO is 709.6 eV; and Fe_3O_4 is 710.3 eV. The binding energy plots verses intensity for the iron oxide layers are shown in Fig. 8. The Fe 2p spectra of FeO and Fe_3O_4 are similar and it is hard to distinguish from each other. The Fe $2p_{1/2}$ and Fe $2p_{3/2}$ binding energy were about 724 and 711.0 eV. It was

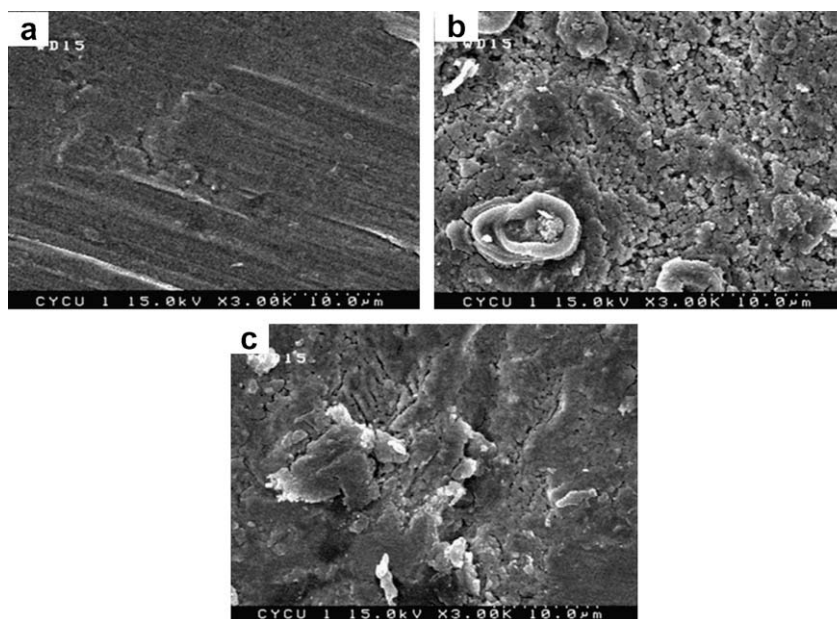


Fig. 7. SEM image for (a) polished, (b) electroactive copolyimide-coated, (c) electroactive polyimide-coated CRS surface.

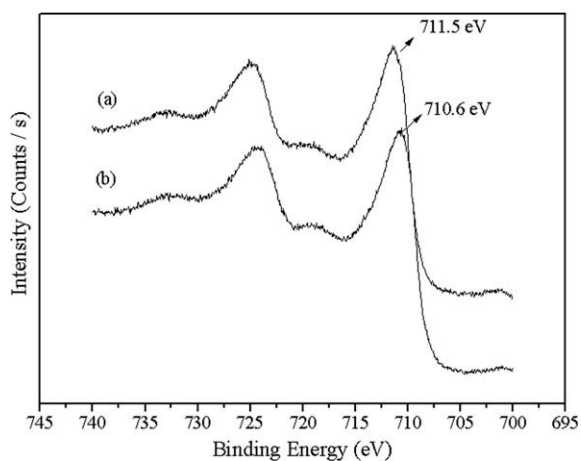


Fig. 8. ESCA Fe 2p core level spectra of (a) electroactive copolyimide, (b) electroactive polyimide.

indicated that the passive oxide layer is predominately composed by Fe_2O_3 , above a very thin Fe_3O_4 layer [40].

4. Conclusions

The electroactivity of as-prepared electroactive polyimide was identified by the cyclic voltammetry (CV) studies. It should be noted that the electroactive polyimide having higher content of aniline trimer exhibited a larger redox current (i.e., higher electroactivity) as compared to that of electroactive copolyimide. However, non-electroactive polyimide showed zero redox current. This implied that the incorporation of ATs into the polyimide may introduce the electroactivity into as-prepared polyimide.

This is the first time that we present evaluations for the effect of ATs on the corrosion protection of as-prepared electroactive polyimide coatings. The as-prepared polyimide with higher content of ATs exhibited obviously enhanced corrosion protection efficiency on CRS electrodes on a basis of a series of electrochemical measurements such as E_{corr} , R_p , I_{corr} and EIS studies. The significant enhancement of corrosion protection on CRS electrodes might probably be attributed to the redox catalytic property of electroactive aniline trimer in the formation of passive layer of metal oxide which was investigated by SEM and ESCA. The iron oxide of the CRS surfaces were studied and found to have a thin layer containing Fe_2O_3 and Fe_3O_4 . The passivation mechanism of electroactive polyimide on the CRS surface is similar to that of polyaniline. The ATs show the excellent corrosion inhibition and acting as a redox catalyst to increase the corrosion protecting ability. These electroactive polyimides are promising anticorrosion materials in many applied fields.

Acknowledgements

The financial support of this research by the Center-of-Excellence Program on Membrane Technology, the Ministry of Education, Taiwan, ROC and NSC 95-2627-M-033-001 is gratefully acknowledged.

References

- [1] Kohlman RS, Joo J, Epstein AJ. In: Mark JA, editor. Physical properties of polymers handbook. New York: American Institute of Physics; 1996. Chapter 34.
- [2] Trivedi DC. in: Nalwa HS, Handbook of organic conductive molecules and polymers, Ed, 1997.
- [3] Ahmed SM, Ahmed SA. Geometrical stability and energy storage of some conducting large aromatic sulfonate-doped polyaniline. Eur Polym J 2001;38(1):25–31.

- [4] Cuentas-Gallegos AK, Lira-Cantú M, Casañ-Pastor N, Gómez-Romero P. Nanocomposite hybrid molecular materials for application in solid-state electrochemical supercapacitors. *Adv Funct Mater* 2005;15(7):1125–33.
- [5] Oshida K, Einaga Y. Photo-control of the electronic states of Iron coordinated to photo-responsive polyaniline. *Thin Solid Films* 2007;515(13):5484–789.
- [6] Kim Y, Yeji K, Teshima K, Kobayashi N. Improvement of reversible photoelectrochromic reaction of polyaniline in polyelectrolyte composite film with the dichloroethane solution system. *Electrochim Acta* 2000;45(8–9):1549–53.
- [7] Brazdziuviene K, Jureviciute I, Malinauskas A. Amperometric ascorbate sensor based on conducting polymer: poly(*N*-methylaniline) versus polyaniline. *Electrochim Acta* 2007;53(2):785–91.
- [8] Xu K, Zhu L, Zhang A, Jiang G, Tang H. A peculiar cyclic voltammetric behavior of polyaniline in acetonitrile and its application in ammonia vapor sensor. *J Electroanal Chem* 2007;608(2):141–77.
- [9] Gupta Y, Hellgardt K, Wakeman RJ. Enhanced permeability of polyaniline based nano-membranes for gas separation. *J Membrane Sci* 2006;282(1–2):60–70.
- [10] Illing G, Hellgardt K, Wakemana RJ, Jungbauer A. Preparation and characterisation of polyaniline based membranes for gas separation. *J Membrane Sci* 2001;184(1):69–78.
- [11] Deberry DW. Modification of the electrochemical and corrosion behavior of stainless steels with an electroactive coating. *J Electrochem Soc* 1985;132(5):1022–6.
- [12] Wessling B. Electrical conductivity in heterogeneous polymer systems (V) (1): further experimental evidence for a phase transition at the critical volume concentration. *Synth Met* 1991;41(3):1057–62.
- [13] Soto-Oviedo MA, Araújo OA, Faez R, Rezende MC, De Paoli MA. Antistatic coating and electromagnetic shielding properties of a hybrid material based on polyaniline/organoclay nanocomposite and EPDM rubber. *Synth Met* 2006;156(18–20):1249–55.
- [14] Mu S. Pronounced effect of the ionic liquid on the electrochromic property of the polyaniline film: color changes in the wide wavelength range. *Electrochim Acta* 2007;52(28):7827–34.
- [15] Yu YH, Lai CY, Chen CL, Yeh JM. Durable electrochromic coatings prepared from electronically conductive poly(3HT-co-3TPP)-silica hybrid materials. *J Electron Mater* 2006;35(7):1571–80.
- [16] Conwell EM, Duke CB, Paton A, Jeyadev S. Molecular conformation of polyaniline oligomers: optical absorption and photoemission of three-phenyl molecules. *J Chem Phys* 1988;88(5):3331–7.
- [17] Shacklette LW, Wolf JF, Gould S, Baughman RH. Structure and properties of polyaniline as modeled by single-crystal oligomers. *J Chem Phys* 1988;88(6):3955–61.
- [18] Rodrigue D, Domingue M, Riga J, Verbist JJ. Electronic structure of polyaniline: experimental study of oligomers. *Synth Met* 1993;57(2–3):4802–6.
- [19] Honzl J, Tlastakova M. Polyaniline compounds. II. The linear oligoaniline derivatives tri-, tetra-, and hexaanilinobenzene and their conductive complexes. *J Polym Sci* 1968;22(1):451–62.
- [20] Lu FL, Wudl F, Nowak M, Heeger AJ. Phenyl-capped octaaniline (COA): an excellent model for polyaniline. *J Am Chem Soc* 1986;108(26):8311–3.
- [21] Cao Y, Li S, Xue Z, Guo D. Spectroscopic and electrical characterization of some aniline oligomers and polyaniline. *Synth Met* 1986;16(33):305–15.
- [22] Wei Y, Yang C, Ding T. A one-step method to synthesize *N,N'*-bis(4'-aminophenyl)-1,4-quinoneimine and its derivatives. *Tetrahedron Lett* 1996;37(6):731–4.
- [23] Wang ZY, Yang C, Gao JP, Lin J, Meng XS, Wei Y, et al. Electroactive polyimides derived from amino-terminated aniline trimer. *Macromolecules* 1998;31(8):2702–4.
- [24] Lu W, Meng XS, Wang ZY. Electrochemical behavior of a new electroactive polyimide derived from aniline trimer. *J Polym Sci Part A: Polym Chem* 1999;37(23):4295–301.
- [25] Chao D, Cui L, Lu X, Mao H, Zhang WJ, Wei Y. Electroactive polyimide with oligoaniline in the main chain via oxidative coupling polymerization. *Eur Polym J* 2007;43(6):2641–7.
- [26] Chao D, Lu X, Chen J, Zhao X, Wang L, Zhang WJ, et al. New method of synthesis of electroactive polyamide with amine-capped aniline pentamer in the main chain. *J Polym Sci Part A: Polym Chem* 2006;44(1):477–82.
- [27] Chao D, Ma X, Lu X, Cui L, Mao H, Zhang WJ, et al. Electroactive hyperbranched polyamide synthesized by oxidative coupling polymerization within an A2+B3 Strategy. *Macromol Chem Phys* 2007;208(6):658–64.
- [28] Chao D, Ma X, Lu X, Cui L, Mao H, Zhang WJ, et al. Design, synthesis and characterization of novel electroactive polyamide with amine-capped aniline pentamer in the main chain via oxidative coupling polymerization. *J Appl Polym Sci* 2007;104(3):1603–8.
- [29] Chao D, Lu X, Chen J, Liu X, Zhang WJ, Wei Y. Synthesis and characterization of electroactive polyamide with amine-capped aniline pentamer and ferrocene in the main chain by oxidative coupling polymerization. *Polymer* 2006;47(8):2643–8.
- [30] Huang L, Hu J, Lang L, Wang X, Zhang P, Jing X, et al. Synthesis and characterization of electroactive and biodegradable ABA block copolymer of polylactide and aniline pentamer. *Biomaterials* 2007;28(10):1741–51.
- [31] Yeh JM, Hsieh CF, Jaw JH, Kuo TH, Huang HY, Lin CL, et al. Organosoluble polyimide (ODA-BSAA)/montmorillonite nanocomposite materials prepared by solution dispersion technique. *J Appl Polym Sci* 2005;95(5):1082–90.
- [32] Yağan A, Pekmez NÖ, Yıldız A. Electrochemical synthesis of poly(*N*-methylaniline) on an iron electrode and its corrosion performance. *Electrochim Acta* 2008;53:5242–51.
- [33] Stern M, Geary AL. Electrochemical polarization. *J Electrochem Soc* 1957;104:56–63.
- [34] Bockris J, Reddy KN. *Modern electrochemistry*. New York: John Wiley and Sons; 1976.
- [35] Park SM, Yoo JS. *Anal Chem A*-pages 2003;75:455.
- [36] Amirudin A, Thierry D. Application of electrochemical impedance spectroscopy to study the degradation of polymer-coated metals. *Prog Org Coat* 1995;26(1):1–28.
- [37] Medrano-Vaca MG, Gonzalez-Rodriguez JG, Nicho ME, Casales M, Salinas-Bravo VM. Corrosion protection of carbon steel by thin films of poly(3-alkyl thiophenes) in 0.5 M H₂ SO₄. *Electrochim Acta* 2008;53(9):3500–7.
- [38] Wessling B. Passivation of metals by coating with polyaniline: corrosion potential shift and morphological changes. *Adv Mater* 1994;6(3):226–8.
- [39] Wessling B. Corrosion prevention with an organic metal (polyaniline): surface ennobling, passivation, corrosion test results. *Mater Corros* 1996;47(8):439–45.
- [40] Lu WK, Elsenbaumer RL, Wessling B. Corrosion protection of mild steel by coatings containing polyaniline. *Synth Met* 1995;71(1–3):2163–6.